One-way and two-way wave-equation migration

W.A. Mulder and R.-E. Plessix, Shell International E&P, The Netherlands

Summary

We present a comparison of results for wave-equation migration in the frequency domain using the constant-density acoustic "two-way" wave equation and its one-way approximation. The examples are based on synthetic and real data for a two-dimensional spatial geometry. In two space dimensions, the two-way approach has a higher computational cost than the one-way method, but not by much. The two-way wave equation provides better imaging of steep flanks. Still, the one-way wave equation gives good results in practice because steep flanks are often poorly illuminated. Migration with the two-way wave equation is sensitive to "turning rays" leading to low-frequency artefacts in the images. These can be removed by blanking of the data or high-pass filtering or iterative migration.

Introduction

We compare results obtained with one-way and two-way finite-difference wave-equation migration for two-dimensional problems. The two-way equation provides a more accurate description of wave propagation in complex media than the one-way equation, but at a higher computational cost. Turn-around times can be reduced by at least one order of magnitude if the frequency instead of the time domain is used (Marfurt and Shin, 1989; Pratt, 1990; Mulder and Plessix, 2002; Plessix and Mulder, 2002a). The higher accuracy of the two-way equation is expected to provide better images of, for instance, steep flanks. In practice, however, these flanks are often poorly illuminated so the advantage is not so clear.

Migration formulas can be derived by starting with the least-squares error functional that measures the difference between synthetic and observed data. The gradient or sensitivity of this functional with respect to the model parameters is a migration image (Lailly, 1983; Tarantola, 1984). To obtain a migration image that is close to true-amplitude, we have constructed and used suitable migration weights by computing an approximation to the diagonal of the Hessian of the error functional with respect to the model parameters (Plessix and Mulder, 2002b). This should be further corrected for the finite-frequency effect of spatial spreading which is related to the size of the Fresnel zone at each scattering point. In two space dimensions, this is accomplished by division of the estimated diagonal of the Hessian by $\sqrt{zv}$, where z is the depth and v the local velocity. In principle, the weighted gradient can be used to update the model parameters repeatedly until the error has decreased to a level where only noise remains. In practice, a good approximation of the migration weights should result in an image that hardly improves after the first migration step, so that iterative migration is not necessary. We will present examples confirming that our migration weights provide correct amplitudes after a single iteration if a regular acquisition geometry is used. Subsequent iterations only improve the focusing of events.

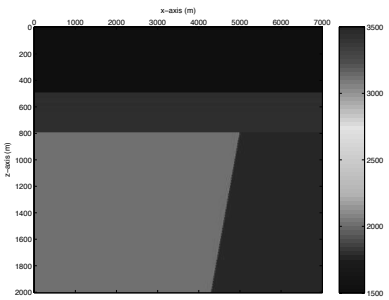

Fig. 1: Velocity model with 60°-dip interface.

The use of the constant-density acoustic wave equation poses a problem for iterative migration. The data are mainly determined by impedance contrasts whereas as the iterative migration can only update velocity contrasts. To circumvent this problem, we have used the Born approximation leading to the use of the *linearized* constant-density acoustic wave equation. In that case, the velocity is kept fixed and velocity perturbations are interpreted as a reflectivity image. These reflectivities become the model parameters for the least-squares problem and are readily computed in a small number of iterations. Examples of this approach can be found in Østmo *et al.* (2002) and more will be shown here.

For the one-way equation, the scheme of Collino and Joly (1995) is used with a three-term Padé approximation, providing good accuracy up to about 70°. The two-way wave equation is efficiently solved in the frequency domain by using a nested-dissection ordering (Marfurt and Shin, 1989; Pratt, 1990). In two space dimensions, one-way and two-way wave-equation migration have roughly the same complexity. Our non-optimal implementation of two-way wave-equation migration required about twice the computer time needed for the one-way equation. In 3D, the complexity of a direct solver for the frequency-domain two-way wave equation is so bad that we either need to find a good iterative solver or will have to return to the time domain (Mulder and Plessix, 2002).

Synthetic data results

The inability of the one-way wave equation to image steep flanks is illustrated by considering a reflector at 40°, 60°, and 80° dip. The velocity model for the 60°-dip interface is shown in Fig. 1. Synthetic data for this and the other two models were generated by the same constant-

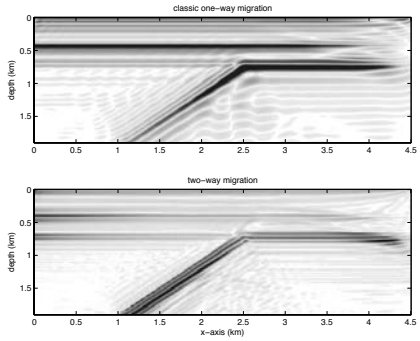

Fig. 2: Migration images for one-way and two-way equation with 40° dip.

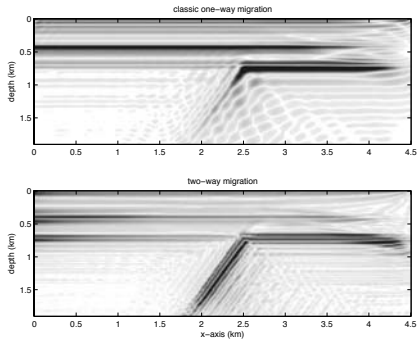

Fig. 3: For 60° dip.

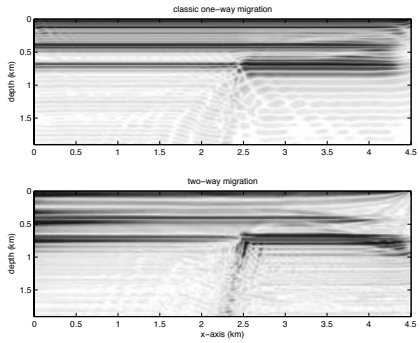

Fig. 4: For 80° dip.

density acoustic frequency-domain code as used for the two-way migration, using frequencies from 8 to 20 Hz with a 0.125 Hz increment. A marine acquisition with 179 shots between 2500 and 6950 m at 25 m distance and 98 receivers per shot at 25 m interval and offsets between −50 and −2475 m was used. The migration results are displayed in Figs. 2–4 for increasing dip angles in the velocity model. The one-way wave equation should provide images that are geometrically similar to the two-way equation for dips up to about 70°. This is confirmed by the images shown. It is well-known that the one-way wave equation does not provide correct amplitudes, as is apparent from the results. At 80° dip, the one-way equation cannot provide a proper image. The two-way equation, however, does not provide a crisp image either due to illumination problems and lack of long offsets.

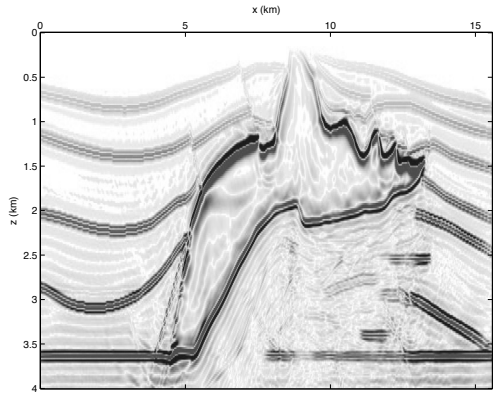

Fig. 5: Migration image for the one-way wave-equation.

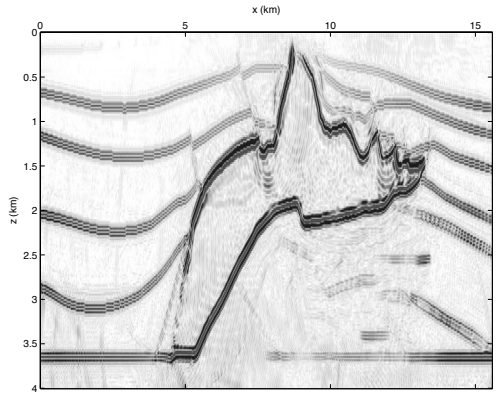

Fig. 6: High-pass-filtered true-amplitude migration image for the two-way wave equation.

The next example is based on the SEG/EAGE AA' salt model (Aminzadeh et al., 1997). Using a time-domain finite-difference code (Mulder and Plessix, 2002), 4 second traces for 237 shots with 65 receivers each were generated. The acquisition geometry mimics a marine acquisition with a shot every 80 m and with a 40 m spacing between receivers. The maximum offset is 2.7 km. The maximum depth in the model used to generate the data is 4.2 km. The direct arrival was blanked before transforming to the frequency domain. Frequencies ranged from 6 to 26 Hz with a 0.25 Hz interval.

The one-way migration image is shown in Fig. 5. Before transforming the data to the frequency domain, linear time-weighting was performed in order to boost the amplitudes of the deeper events. The two-way true-amplitude result is shown in Fig. 6. In this case, no time-weighting of the data was applied. The last image has been high-pass filtered to remove artefacts caused by the equivalent of "turning rays", to be discussed in more detail in the next examples. The two-way equation provides a better image of the steep flanks in the shallow part of the model, whereas some of the structures below the salt are clearer.

Princess results

We have used a data set from an area called Princess in

the Gulf of Mexico as a real-data example. One out of six streamer lines was selected from a 3D data set. NMO stacking of several lines in the cross-line direction was applied to make the data more or less two-dimensional. Shot and receivers are spaced at 25 m with a maximum offset of 8.3 km. The velocity model is displayed in Fig. 7. The migration result obtained with the one-way equation is presented in Fig. 8. The data have been time-weighted by t^2 before transforming them to the frequency domain. We have use frequencies from 6 to 30 Hz at a 0.125 Hz increment. The migration weights based on the Hessian were *not* applied. Figure 9 shows a true-amplitude two-way migration image using the same data up to 20 Hz, but without time weighting and with the Hessian applied. There are artefacts with a spatial low frequency causes by "turning rays". These can be removed in several ways.

One approach is the application of a high-pass filter. We have constructed a simple filter based on convolution with $\{\frac{1}{4}, \frac{1}{2}, \frac{1}{4}\}$ in each coordinate direction. This convolution is denoted by S_x for the x- and by S_z for the z-direction. We let $S = S_z S_x$. The term $[n_1, n_2, n_3]$-filter will be used for the operator $S_x^{n_3} S^{n_2}(I - S^{n_1})$, where I is the identity operator. This amounts to high-pass filtering by smoothing an image n_1 times and subtracting the result, followed by smoothing the result n_2 times and another n_3 times in only the x-direction to reduce noise. Figure 10 shows the result of applying a $[64, 0, 8]$ filter to Fig. 9. This reduces the artefacts but does not completely remove them. The $[32, 0, 2]$ filter used below does a better job but also removes some of the reflectors.

A second approach is the removal of the "turning-ray" events from the data, which is quite difficult in general. If we simply blank the data for $t < 0.2 + 0.00109\,h$, where t is time in seconds and h is offset in meters, we obtain the result shown in Fig. 11, using frequencies from 6 to 20 Hz with a 0.125 Hz increment. Now most, but not all of the artefacts have been removed.

A third approach is to apply iterative migration (Østmo, S, Mulder, W.A., and Plessix, R.-E, 2002). The result after 6 iterations for 6 to 20 Hz with a 0.25 Hz increment, is displayed in Fig. 12. The artefacts are weaker but have not been completely removed. For comparison, we have included high-pass filtered pictures of the first and sixth iteration using a $[32, 0, 2]$ filter. Comparison of Fig. 13 and Fig. 14 shows that the iterations have little effect on the reflectors themselves. This means that our migration weights do quite a good job. If they would not, the amplitudes would change markedly from one iteration to the next.

Conclusions

The comparison of migration results for one-way and two-way wave-equation migration shows that the two-way wave equation provides better results for steeper dips. In practice, this advantage is less clear, because steep dips are often poorly illuminated. A disadvantage of the two-way wave-equation migration is the occurrence of the equivalent "turning rays", producing artefacts of low spatial frequencies. These can be removed by a high-pass spatial filter. Alternatively, the corresponding events can be blanked from the data but this may be difficult. Iterative migration will reduce the amplitude of the artefacts and will generally improve the amplitude and focusing of the reflectors, but this will increase the computational cost.

Acknowledgements

The authors thank the management of Shell Exploration & Production Company (SEPCo) for permission to use the Gulf of Mexico data.

References

Marfurt, K. J., and Shin, C.S., 1989, The future of iterative modeling in geophysical exploration, in E. Eisner, Ed., Supercomputers in seismic exploration, Pergamon Press.

Pratt, R.G., 1990, Frequency-domain elastic wave modeling by finite differences: a tool for crosshole seismic imaging, Geophysics, **55**, 626–632.

Mulder, W.A., and Plessix, R.-E., 2002, *Time- versus frequency-domain modelling of seismic wave propagation,* Extended Abstract E015, 64th EAGE Conference & Exhibition, Florence, Italy.

Plessix, R.-E., and Mulder, W.A., 2002, How to choose a subset of frequencies for frequency-domain finite-difference migration, Extended Abstract A038, 64th EAGE Conference & Exhibition, Florence, Italy.

Lailly, P., 1983, *The seismic inverse problem as a sequence of before stack migration*, In Proc. of Conf. on Inverse Scattering, Theory and Applications, SIAM, Philadelphia.

Tarantola, A., 1984, Linearized inversion of seismic reflection data, Geophys. Prosp., **32**, 998–1015.

Plessix, R.-E., and Mulder, W.A., 2002, Amplitude-preserving finite-difference migration based on a least-squares formulation in the frequency domain, Extended Abstract MIG 4.3, SEG International Exposition and 72nd Annual Meeting, Salt Lake City, Utah.

Østmo, S, Mulder, W.A., and Plessix, R.-E., 2002, Finite-difference iterative migration by linearized waveform inversion in the frequency domain, Extended Abstract MIG P1.6, SEG International Exposition and 72nd Annual Meeting, Salt Lake City, Utah.

Collino, F, and Joly, P., 1995, Splitting of operators, alternate directions, and paraxial approximations for the three-dimensional wave equation, SIAM J. Sci. Comput., **16**, 1019–1048.

Aminzadeh, F., Brac, J., and Kunz, T., 1997, 3-D Salt and Overthrust Models, Soc. of Expl. Geophysicists.

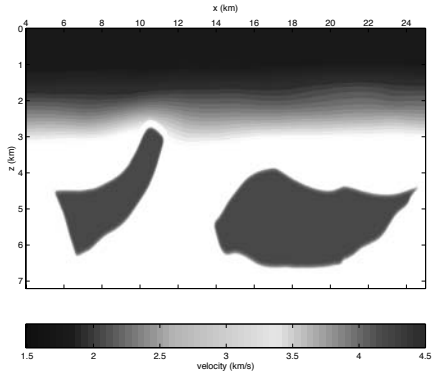

Fig. 7: Princess velocity model.

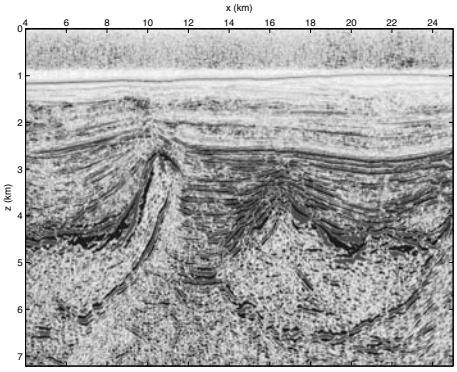

Fig. 8: One-way migration result.

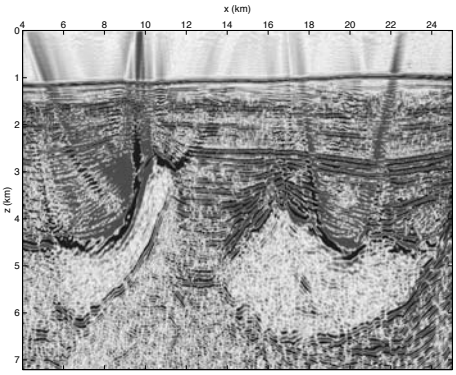

Fig. 9: True-amplitude migration image.

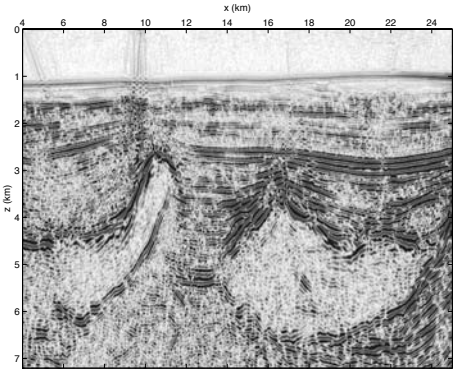

Fig. 10: Filtered true-amplitude migration image.

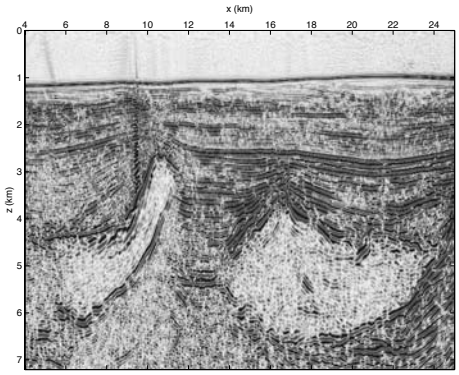

Fig. 11: True-amplitude image based on blanked data.

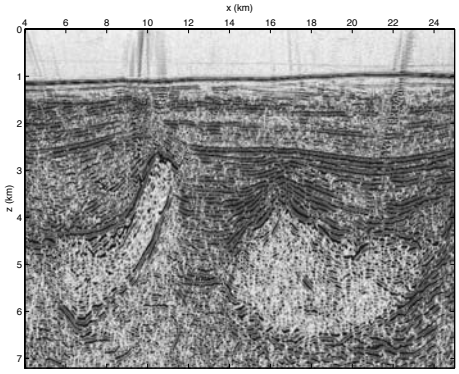

Fig. 12: Migration result after six iterations.

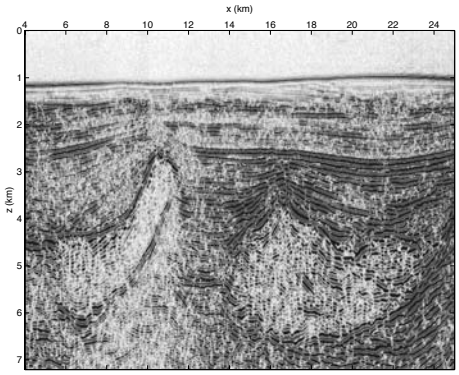

Fig. 13: First iteration, high-pass filtered.

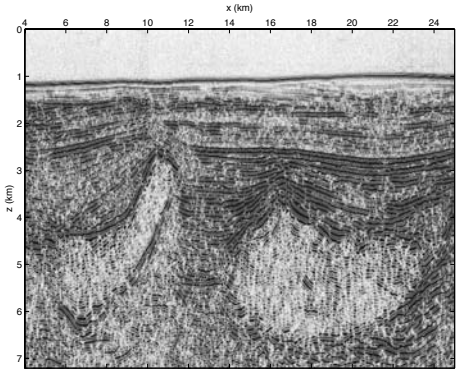

Fig. 14: Sixth iteration, high-pass filtered.